Integrity of Bored Piles Under Tension

Orhan E. İnanır [i] and Müge İnanır [ii]

i) Technical Manager, GEOgrup A.S., No:30/28, Meric Cad, İstanbul 34750, Türkiye.

ii) Managing Director, GEOgrup A.S., No:30/28, Meric Cad, İstanbul 34750, Türkiye.

ABSTRACT

Instrumented pile loading tests can give a better understanding about the pile load-transfer mechanism. It gives also opportunity to assess the integrity and durability issues of the bored pile under tension. When a reinforced concrete bored pile subjected to high tension forces, it might reaches to tensile stress capacity of concrete and cracking occurs at a weakest section. The formation of cracks influences the load-displacement behaviour of piles under tension load and it causes difficulties during interpretation of pull-out tension test results. The full shaft resistance capacity can only be taken into account when it reaches the required relative displacement along the pile for fully mobilized shaft resistance and crack deformation. Especially for long piles this cannot be achieved in the acceptable pile displacement range. Thus there are different tendencies in various design manuals to limit the pile capacity under tension by applying higher safety factors or by lowering the resistance factors. However, these approaches might not always guarantee crack free design under service load.

In this study an instrumented pile pull-out tension test results are briefly presented from crack formation and propagation aspect. Crack opens when the tensile deformation from applied loads reaches the tensile deformation capacity of concrete (Borosnyoi and Balazs, 2005, Bicocchi, 2011). In addition to this study, authors have also experienced between 50-150 microStrain values for crack formation at piles during pull-out tension test with different concrete characteristics and different steel content (Inanir, 2018). Bicocchi, (2011) also reported similar findings with strain gauge measurements while flexural bending crack formation at piles. The position of the SG and the influence zone of the cracked section might affect the measured value during first crack formation.

It might also be a good practice in design to limit the elongation of reinforced concrete body of the pile which is subjected to tension. In other words limiting the mobilized strain (between 50-100μstrain) in the pile for crack free design might ensure an improved pile performance and material durability, but on the other hand this is preventing from taking advantage of the reinforcement tensile capacity.

Keywords: integrity, crosshole logging, tension, crack, pull-out, instrumented pile loading test

1 INTRODUCTION

Instrumented pile loading tests can give a better understanding about the pile load-transfer mechanism. It gives also opportunity to assess the integrity and durability issues of the bored piles under tension. When a reinforced concrete bored pile subjected to high tension forces, it might reach to tensile stress capacity of concrete and cracking occurs at a weakest section.

It is reported by Fellenius (2021) and England (2012) that the direction of the movement has no effect for the shaft resistance, in other words the shaft shear stress absolute values are the same if the pile is under compression or tension load. On the contrary there are also studies indicating that under same soil conditions the shaft resistance in tension (pull-out resistance) is less than the shaft resistance in compression (Jardine et.al., 1996, Liew et.al., 2011).

Jardin et.al. (1996) reported smaller radial effective stress and peak local shear stress under tension on the shaft of piles compared to compression loading in sand. However no difference in clay.

Liew et.al. (2011) reported reduction in shaft resistance which is dominated by the pile radial shrinkage from the poisson ratio effect under tension. Moreover, they reported also that they observed signal delay in first arrival time (FAT) and decrease of signal energy (E) at crosshole logging test during pull out tension test due to tension crack formation.

In this study an instrumented pile pull-out tension test results are briefly presented from crack formation and propagation aspect. Crack opens when the tensile deformation from applied loads reaches the tensile deformation capacity of concrete (Borosnyoi and Balazs, 2005; Bicocchi, 2011). The crack formation is a complex process that primary and secondary crack formations controls the stress-strain behaviour of the reinforced concrete structure.

This mechanism was studied by Somayaji and Shah, (1981) and was described with three region on a typical load-strain curve of reinforced concrete members subjected to tension (Fig.1a.). First region represents the elastic behaviour of the member up to start of primary cracking. Second region covers deformation behaviour from the first primary crack to the final cracking point. Third region represents the behaviour from the final cracking point to the yielding of the reinforcement.

Fields and Bischoff (2004) identified axial stress and strain distribution along the reinforced concrete members subjected to tension (Fig.1b.) When the stress in concrete first reaches the tensile strength at a weakest section, cracking occurs. After cracking, the stress in the concrete at the crack drops to zero. The concrete stress increases with distance from the crack due to the bond action, until at distance called the transfer length (s), from the crack the concrete stress is not affected by the crack, as shown in Fig. 1b. Slip at the concrete steel interface in the region of significant bond stress causes the crack to open. A relatively small increase in load will cause a second crack to develop at a cross-section at some distance from the first crack. While the load is increasing, the primary cracks form at somewhat regular intervals ($s<l\leq(2\cdot s)$, Fig. 1b) propagating along the member and primary crack pattern is established. The concrete tensile stress at each crack is zero, rising to a value σ_{ct}, which never reaches the tensile strength of the concrete (Fig. 1b).

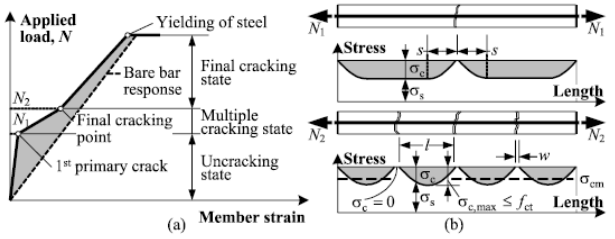

Fig. 1. (a)Tension member: cracking stages (Somayaji and Shah 1981) and (b) distribution of axial stresses and strains (Fields and Bischoff 2004)

The above mentioned phenomenon was observed from the strain gauge data which had been collected during the pull-out tension test. In addition, in order to justify the development of cracks along the pile, crosshole logging and sonic integrity tests were conducted on bored pile before, at maximum load and after pull-out tension test.

2 SUBSURFACE CONDITION

Man-made fill extending up to 4m below the ground surface is encountered at the project test site. Below man-made fill, there are sandstone and mudstone alternating layers till the end of the borehole. The ground water level is located close to the surface. The test site was excavated up to 16m depth (EL -13.30) and ground water table was lowered to EL=-13.30 prior to pull-out tension test. The soil profile summary info is given at Table 1.

Table 1. Ground conditions.

Elevation (m) GRS80	Material Description
+2.7 / +0.0	Man-made fill: Rock Boulders with brick fragments, sand and clay
+0.0 / -0.7	Man-made fill:Sandy clay with rock fragments
-0.7 / -1.2	Man-made fill: Rock boulders
-1.2 / -9.6	Sandstone
-9.6 / -12.4	Mudstone
-12.4 / -20.2	Sandstone
-20.2 / -23.3	Stratified Mudstone
-23.3 / -23.8	Conglomerate
-23.8 / -24.5	Sandstone

3 TEST PILE AND INSTRUMENTATION DETAILS

3.1 Pile installation

The test pile, which was Φ1000mm in diameter and L_{total}=10.40m in length, was constructed from working platform elevation (EL -13.10) by drilling soft to medium rock using rock auger attachment. Temporary casing (L=6m, OD1080mm) was used during drilling and upon reaching to the full depth the reinforcement cage (22nosΦ32mm main rebar with Φ12/100mm spiral) was inserted into the hole (Fig.2).

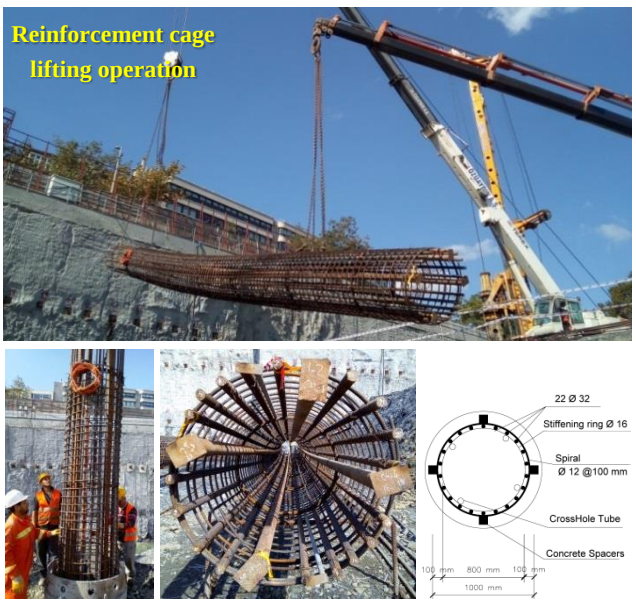

Fig. 2. General views from the pile installation and reinforcement cage detail.

Strain gauges, GI pipes for telltale rods and steel tubes for crosshole logging test (CSL tubes were also used for later insertion of retrievable extensometers, EXT2strain) were installed to the reinforcement cage and the concrete was placed by tremie method.

3.2 Instrument Installation

Along the test pile, four (4) levels of sister bar type vibrating wire strain gauges (VWSG/S) were installed and at each level there were four (4) units of VWSG/S for redundancy. Strain gauge depths were 1.2m (SG1), 3.7m (SG2), 6.9m (SG3) and 9.4m (SG4) from the pile head (Fig.4.). In addition to strain gauges, two (2) nos retrievable extensometer EXT2strain arrays were installed along the two CSL tubes, which were 180 degrees apart, for measuring elongation (average strains) between 2nosx6 level anchor points. Also, two (2) nos telltales installed at the pile toe, which were again 180 degrees apart, for measuring the pile toe movement.

As the residual stresses were not taken into account, the strain gauge readings zeroed at the beginning of the test.

General views for instrumentation details and schematic representation of gauge levels along the pile are given at Fig.3 and Fig. 4.

Fig. 3. General views from the instrumentation detail.

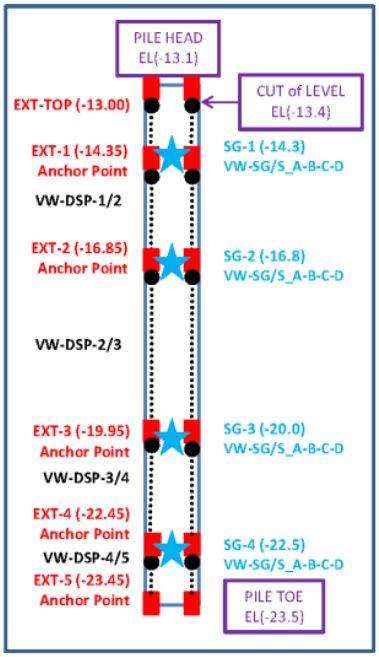

Fig. 4. Schematic representation of VW sister bar strain gauges and EXT2strain levels along the pile.

3.2 Loading test

The tension load was transferred to the pile head with a load transfer pipe which is welded to the main reinforcement bars of the test pile. A reaction beam was seated on the reaction piles which were acting against pulling forces of the test pile. The schematic and general views are shown in Fig. 5. and Fig. 6.

Loading test was commenced by applying pressure to the hydraulic jacks using an air-driven hydraulic pump. A high-pressure Bourdon gauge as well as a calibrated pressure transducer was used to measure the pressure. Transferred load to the pile head was measured by an electric resistive solid load cell. The displacement transducers, which were supported from the reference beam, were used to measure relative movements at the designated points of measurement. Leica DNA-03 automatic level was used for monitoring the reference beam movement during the test. Invar leveling rod was attached to the reference frame and to fixed control station for reference.

The loading test was performed in accordance with ASTM D 3689-07 (2013) specification and Procedure A "Quick Test" schedule was followed by applying small and approximately equal increments of load at equal relatively short time intervals. The maximum load 7.7 MN was reached through 22 loading steps by applying %5 of the test load at each step with 15 minutes loading duration as given in Fig.7. Unloading was completed with 5 intervals after waiting for 1 hour at maximum load. Finally the test was completed after waiting for 1 hour at zero load. Throughout the test the displacement, load and strain data were automatically recorded at 60 seconds interval with Automatic Data Acquisition System.

Table 2. Pile loading test summary information.

Maximum Test Load:	7.642 kN (Tension)
Test Pile:	D=1.000mm, L_{net}=10.4m
Reaction Type:	Static Axial Tensile Loading Test *(load transferred with reaction piles)*
Hydraulic Jacks:	Hydraulic jack with 800 ton capacity
Load Cell:	Encardio-Rite ELC-150S-H High Capacity Resistive Type Solid Load Cell *1no x 12.5 MN*
Displacement Gauges:	Opkon SLPS100, 100mm stroke, resistive potentiometer *(4 nos at pile head, 4 nos at welding pipe, 2 nos at Telltale, 1 nos at jack opening—Total 11nos)* Geokon Vibrating Wire Displacement Transducer (VW-DT) 25mm stroke *2 ea/level x 5 level =10 nos VW-DT*
Strain Gauges:	Encardio-Rite EDS-12V Sister Bar Type Vibrating Wire Strain Gauge *4ea/level x 4 level = 16nos* Geokon A9 Model "Retrievable Extensometer" EXT2strain *2 ea/level x 6 level =12 nos anchor point*
Pressure Gauge:	Wika S-10 *1no Pressure Transducer*
Data Rec. Equip:	RST Instruments Flexdaq Logger *1no Campbell Scientific CR6*
Data Rec. Intr:	60 seconds

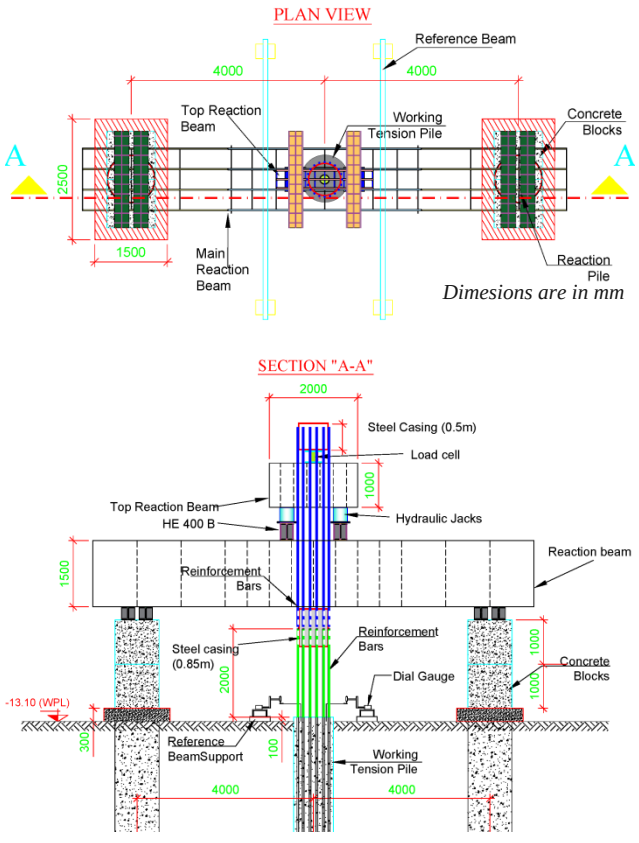

Fig. 5. Schematic view of pile test setup.

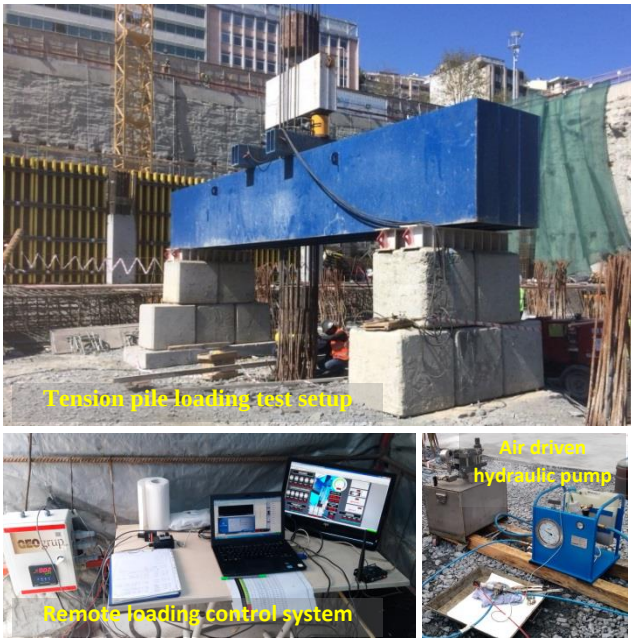

Fig. 6. General views from test setup, loading and measurement system.

Loading Cycle			Pump Pressure (Bar)	Test Load (kN)	Percent of required max. test load (%)	Load Holding Criteria: Loading Duration (Minute)	Load Holding Criteria: Rate of Creep to be obtained
1	L-	0	0	0	0	0	
1	L-	1	34	349	5	15	
1	L-	2	69	698	10	15	
1	L-	3	104	1046	15	15	
1	L-	4	138	1395	20	15	
1	L-	5	173	1744	25	15	
1	L-	6	207	2093	30	15	
1	L-	7	242	2441	35	15	
1	L-	8	277	2790	40	15	
1	L-	9	311	3139	45	15	
1	L-	10	346	3488	50	15	
1	L-	11	381	3836	55	15	
1	L-	12	415	4185	60	15	
1	L-	13	450	4534	65	15	
1	L-	14	484	4883	70	15	N/A
1	L-	15	519	5231	75	15	
1	L-	16	554	5580	80	15	
1	L-	17	588	5929	85	15	
1	L-	18	623	6278	90	15	
1	L-	19	658	6626	95	15	
1	L-	20	692	6975	100	15	
1	L-	21	727	7324	105	15	
1	L-	22	761	7673	110	60	
1	U-	1	692	6975	100	15	
1	U-	2	554	5580	80	15	
1	U-	3	415	4185	60	15	
1	U-	4	277	2790	40	15	
1	U-	5	138	1395	20	15	
1	U-	6	0	0	0	60	

Fig. 7. Loading test schedule.

3.3 Low strain integrity test and crosshole logging on test pile

Low strain integrity test (sonic integrity / pulse echo test) was performed as per ASTM D5882.16 (2016) with Piletest made PET-BT equipment. Crosshole logging test was performed as per ASTM D6760.16

(2016) on tension pile (Φ1000mm diameter and L=10.4 m) with Piletest made CHUM equipment. To assess the pile integrity, both integrity and crosshole logging tests were performed prior to pull-out tension test, during maximum loading and after unloading (Fig.8.). Repeated crosshole logging tests, at maximum load and after unloading, were only done at between no. 2-4 CSL tubes, as the other CSL tubes (no.1-3 CSL tubes) were utilized with retrievable extensometer EXT2strain during the pull-out tension test.

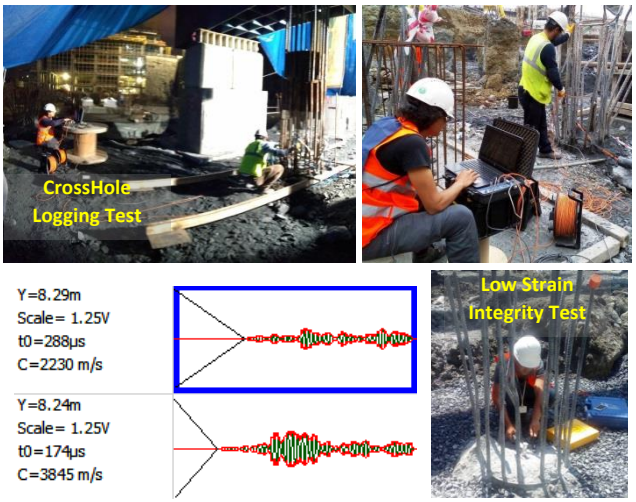

Fig. 8. General views from low strain integrity and crosshole logging test.

4 PILE LOADING TEST RESULTS

4.1 Load-movement behaviour of test pile

The pull-out tension test was performed 28 days after construction. The pile head upward averaged movement at maximum load was 34.90mm, and upward averaged movement of the pile toe was 30.61mm (Fig. 9.). The slope of Load-Upward Movement graph shows that before "Distinctive Yield Point" the axial rigidity is remarkably higher compared to the axial rigidity beyond (Fig.9a.).

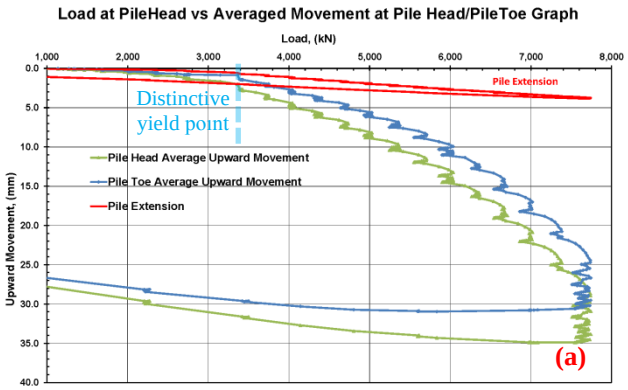

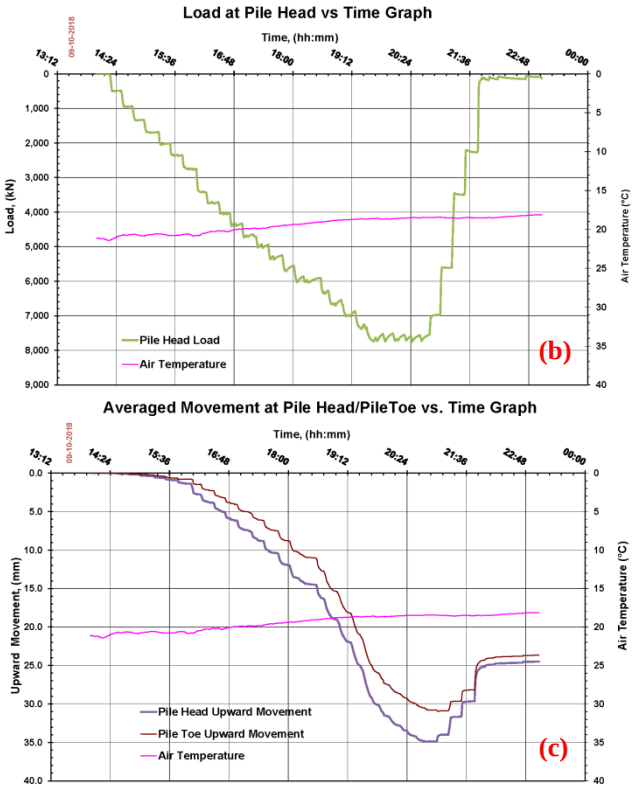

Fig. 9. Test pile (a) load at pile head vs. average movement at pile head and pile toe (b) load at pile head vs. time (c) average movement at pile head and pile toe vs time graphs.

4.2 Strain data along the test pile

The strains induced by the loading of the pile head are shown in Fig. 10 for both strain gauge data and average strain between anchor points for EXT2strain data. Strain gauge data shows sharp strain change compared to EXT2strain data. Jump in the graph can be considered to indicate a first crack formation. Crack formation was detected at SG-1 level (1.2m deep) at approx. 2.3 MN pile head load level and at around ~70 microStrain tensile deformation. As expected, at this load level, the largest strain was observed at SG-1 whereas less strain was observed at the deeper gauge levels. The crack propagation could be seen at SG-2 and SG-3 levels (3.7m and 6.9m deep) approx. at 3.4 MN and 5.0 MN further pile head loads and at around ~120 and ~70 microStrain tensile deformation respectively as shown in Fig. 10a. However, above mentioned observations could not be clearly detected from the EXT2strain data due to using the average strain between anchor points. It is obvious that SG strain gauge measurement indicates locally very high strain values close to the cracked or transition zone, while EXT2strain (retrievable extensometer) measures the displacement between anchor points and strain is calculated accordingly, which gives average strain between anchor points along the pile.

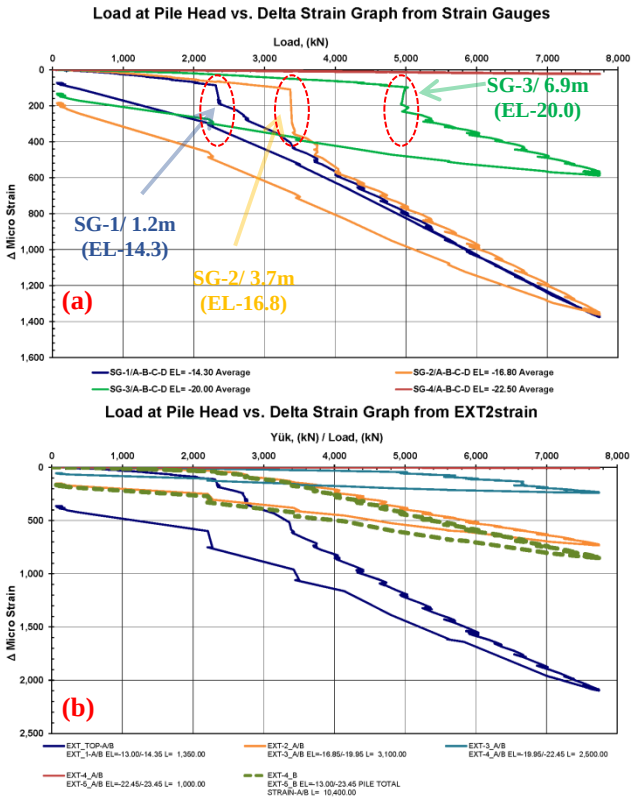

Fig. 10. Test pile (a) load at pile head vs. strain data from VWSG/SB (b) load at pile head vs. strain data from EXT2strain.

4.3 Low strain integrity and crosshole logging test results prior, during and after pile loading test

The measured duration of the hammer blow for low strain integrity test is rather long ~2m . The use of a smaller hammer with shorter duration (0.5 – 1m) would have been better to detect cracks in the pile (Middendorp, et.al. 2006.).

According to the reflectogram (average of >10 nos repeatable blows), which is gathered prior to loading test, a clear toe reflection approximately at 10.50m and the temporary casing penetration depth at approximately 5.5m is also detectable with given test parameters in Fig.11.

During the maximum loading, there is a high shaft friction mobilized along the pile. Due to high shaft friction and cracks there are various reflections and these cause difficulty for the interpretation of the reflectogram. After unloading there might be slight residual shaft friction locked along the pile. However this locked forces are not comparable with the maximum load level.

As can be seen from the reflectogram, at the end of pull-out tension test, it gives detectable "FreeEnd" reflection around 1.5m and repeating peaks (apprx. 3.0m, 4.5m, etc). It might be considered as anomaly/flaw and this is most likely because of cracks.

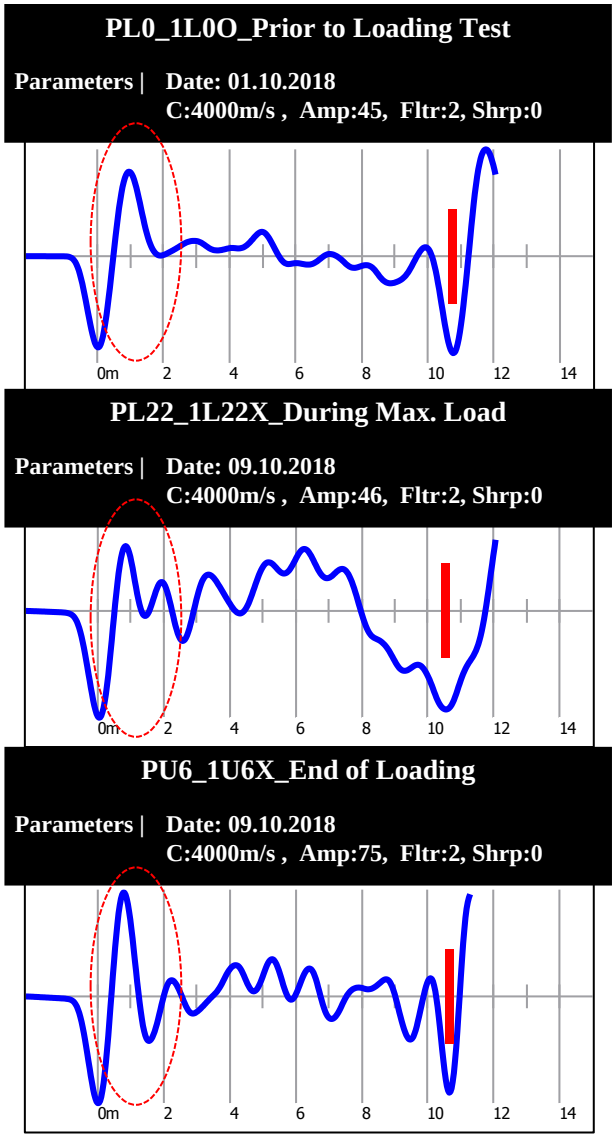

Fig. 11. Test pile low strain integrity test reflectograms (a) prior to loading test (b) at maximum load (c) after loading test.

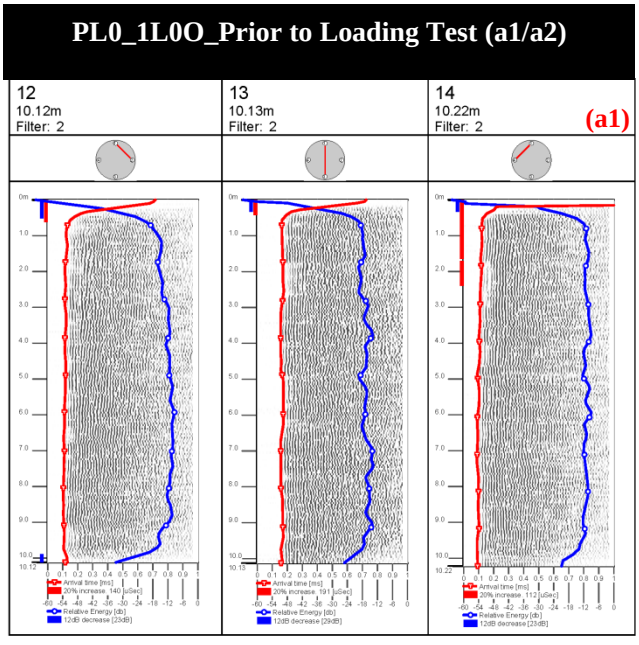

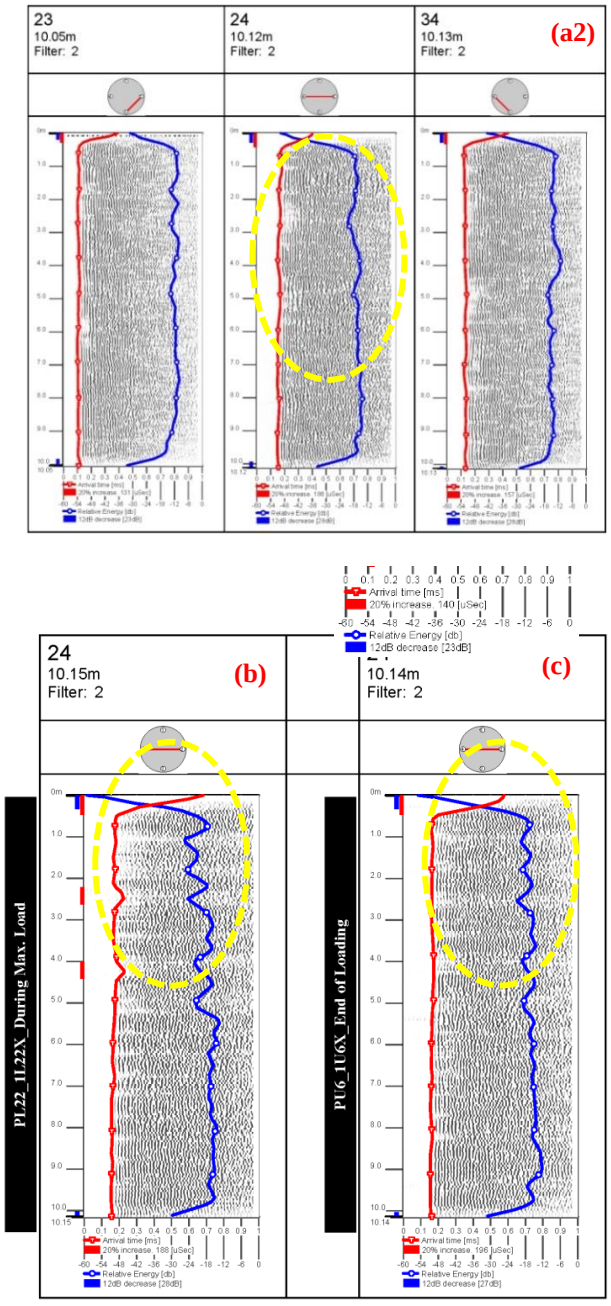

Fig. 12. Test pile crosshole logging graphs (a1/a2) prior to loading test (b) at maximum load (c) after loading test.

Crosshole logging tests were performed with standard scan method. If "offset scan" by positioning emitter and receiver to different depths or 3-D tomography was performed, the crack formation might be better presented. But still it was measured >20% FAT delays (with an amplitude insensitive special FAT detection algoritm, Amir and Amir, 1998) and ~7dB Energy reduction ($6dB<E_{reduction}<9dB$) close to the SG positions. These values correspond to P/F (Poor/Flaw) shaft evaluation scale which is recommended by Likins et.al.(2007).

These anomalies/flaws are most likely because of cracks and can be evaluated as supporting evidences for SG measured crack availability at that levels.

5 INTERPRETATION OF TEST RESULTS

The cracking process can be considered mainly in two parts: crack formation and stabilised cracking (Fig.1.). During the first phase, cracks form at random locations according to the areas of weaknesses where the tensile strength of concrete is exceeded. After the formation of the crack, the tensile forces are carried by the reinforcement in the section and concrete stresses drop to zero (compatibility of strains between concrete and reinforcements is no longer maintained) [Borosnyoi and Balazs (2005)]. Along the pile, moving away from the crack, the tensile stresses in the concrete increase as load is transferred by bond stresses between the concrete and reinforcements. At a certain distance (termed the transfer length), compatibility of strains is recovered again. In the crack formation phase, the zones in which strain compatibility applies are independent of each other. With increasing load new cracks may be formed and the average crack spacing is decreased [Borosnyoi and Balazs (2005)]. The stabilised cracking phase is reached when practically no more new cracks can be formed; the cracks are so close to each other that there is insufficient distance between them for the concrete stress to reach the value corresponding to cracking space. In this phase the average crack spacing remains constant and an increase in load causes an increase of crack width only [Borosnyoi and Balazs (2005)]. This means that all the tensile stresses are effectively carried by the reinforcement.

SG measured data is the primary evidence for crack formation. The flaws at low strain integrity and crosshole sonic logging data are most likely because of these cracks and can be evaluated as supporting evidences. The strain versus load at pile head relation shows approx. 70-120 microStrain range where concrete starts to crack as shown in Fig.13.

According to the ACI 318-14 manual (2014), the relationship between concrete elastic modulus and unconfined compressive strength can be given for normal-weight concrete as follows;

$$E_{CONC} = 4{,}700 * \sqrt{(f'_c)}\ (MPa) \qquad (1)$$

E_{conc}= Concrete elastic modulus
f'_c = Concrete test cylinder unconfined compressive strength

Cyclinder unconfined compressive strength (28 days) was reported as 29.9 MPa for the test pile. Concrete elastic modulus can be derived as 25.7 GPa. By including net concrete cross section EA_{conc} (MN), axial rigidity 19.7 GN can also be calculated. For the composite axial rigidity calculation, 22nosΦ32mm main rebar contribution should be included (E=210GPa, A=17.693mm^2) as $EA_{reinfrc}$=3.7 GN. The calculated composite total axial rigidity (concrete and reinforcement) corresponds to EA_{comp}=23.4 GN.

SG-1 level (1.2m deep) could be accepted as unaffected by shaft resistance. Incremental changes in

pile head test load, results in proportional incremental internal force increases at the strain gage level. The slope of the strain variation versus pile head load for SG-1 data for contact zone can be calculated as 21.4 GN and cracked zone can be calculated as 4.7 GN from Fig. 13. Those values are comparable with calculated axial rigidities of composite cross section and reinforcing rebar respectively.

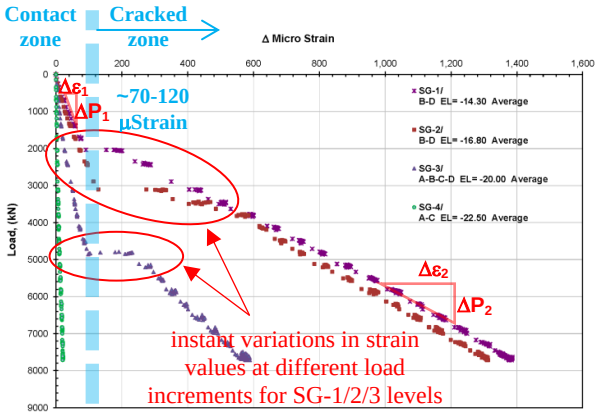

Fig. 13. Strain variation for different SG levels vs. load at pile head graph

6 CONCLUSIONS

When a reinforced concrete bored pile subjected to high tension forces, it might reaches to tensile stress capacity of concrete and cracking occurs at a weakest section. SG measured data is the primary evidence for crack formation during pull-out tension test. The flaws at low strain integrity and crosshole sonic logging data are most likely because of these cracks and can be evaluated as supporting evidences.

Moreover, beside direct observed evidences, axial rigidity calculations are also in line. Concrete-rebar composite cross section dominates the pile axial rigidity at contact zone but at the cracked zone only reinforcement rebar controls the pile axial rigidity. This causes yielding effect on load-movement behaviour of the reinforced concrete bored piles which are subjected to tension. The change in the pile material behaviour affects the pile capacity calculations although it is not because of the pile shaft resistance.
This phenomenon was observed in the tensile deformation range of 70-120µstrain. It might also be a good practice in design to limit the elongation of reinforced concrete body of the pile which is subjected to tension. In other words limiting the mobilized strain (50-100µstrain) in the pile for crack free design might ensure an improved pile performance and material durability, but on the other hand this is preventing from taking advantage of the reinforcement tensile capacity.

Additional researches are required to understand more for crack formation and tensile strain effect on pile design for reinforced concrete bored piles subjected to tension.

REFERENCES

1) ACI Committee, American Concrete Institute, International Organization for Standardization (2014): Building Code Requirements for Structural Concrete (ACI 318-14) and Commentary. American Concrete Institute.
2) Amir, E.I and Amir J.M. (1998). Recent Advances in Ultrasonic Pile Testing, Proc. 3rd Intl' Geotechnical Seminar on Deep Foundation On Bored and Auger Piles, Ghent, pp. 181-185
3) ASTM D3689/D3689M-07, (2013) e1. Standard Test Methods for Deep Foundations Under Static Axial Tensile Load, ASTM International, West Conshohocken, PA, 2016, www.astm.org
4) ASTM D5882-16, (2016). Standard Test Method for Low Strain Impact Integrity Testing of Deep Foundations,
5) ASTM D6760-16, (2016). Standard Test Method for Integrity Testing of Concrete Deep Foundations by Ultrasonic Crosshole Testing.
6) Bicocchi, N., (2011). Structural and Geotechnical Interpretation of Strain Gauge Data from Laterally Loaded Reinforced Concrete Piles, phD Thesis, University of Southampton.
7) Borosnyoi, G. and Balazs, G. (2005). Models for flexural cracking in concrete: the state of the art, Structural Concrete 6 No 2: 53-62.
8) Likins, G. E., Rausche, F., Webster, K. and Klesney, A. (2007). ''Defect Analysis for CSL Testing''. Geo-Denver 2007 New Peaks in Geotechnics.
9) England, Melvin. (2012). On the Subject of Piles in Tension. 680-693. 10.1061/9780784412084.0047.
10) Fellenius, B.H., (2021). Basics of Foundation Design, Electronic Edition, www.Fellenius.net.
11) Fellenius, B.H. (1989). Tangent Modulus of Piles Determined from Strain Data. ASCE, Geotechnical Engineering Division, the 1989 Foundation Congress, F.H. Kulhawy, Editor, Vol. 1, pp. 500-510.
12) Fields, K. and Bischoff, P. H. (2004). Tension stiffening and cracking of high-strength reinforced concrete tension members, ACI Structural Journal 101(4): 447–456.
13) Inanir, O.E. (2018) Load Transfer Behaviour of Axial Loaded Piles and Integrity of Bored Piles which are Subjected to Tension Load, FC-TUGM Symposium `Teoriden Uygulamaya Geoteknik Mühendisliği Sempozyumu`, İstanbul University 10=05=2018, 92-106 (In Turkish).
14) Jardine, R.J. and Chow, F.C.(1996). New design methods for offshore piles. MTD Publication 96/103, MTD, London.
15) Liew, S.S., Khoo, C.M. and Tan, S.T. (2011). Pile Performance in Weathered MetaSedimentary Formation and KL Limestone. Corpus ID: 198924708, Malaysia.
16) Middendorp, P., Schellingerhout, J., (2006). Pile Integrity Testing in the Netherlands. 10th International Conference on Piling and Deep Foundations, DFI , Amsterdam.
17) Somayaji, S. and Shah, S. P. (1981). Bond stress versus slip relationships and cracking response of tension members, ACI Journal Proceedings 78(3): 217–225.
18) Wu, H. Q. and Gilbert, R. I. (2008). An Experimental Study of Tension Stiffening in Reinforced Concrete Members under Short-Term and Long-Term Loads. UNICIV Report No. R-449. Sydney: The University of South Wales. 32 p.